Appl. Chem. Eng., Vol. 35, No. 4, August 2024, 352-359
https://doi.org/10.14478/ace.2024.1036

Article

Adsorptive Removal of Cu(II), Pb(II), and Hg(II) Ions from Common Surface Water Using Cellulose Fiber-Based Filter Media

Phani Brahma Somayajulu Rallapalli and Jeong Hyub Ha†

Department of Integrated Environmental Systems, Pyeongtaek University, Pyeongtaek 17869, Republic of Korea
(Received June 25, 2024; Revised July 10, 2024; Accepted July 11, 2024)

Abstract

Environmental pollution from heavy metal ions (HMIs) is a global concern. Recently, biosorption methods using cellulose sorbents have gained popularity. The objective of this study was to assess the removal efficiency of Cu(II), Pb(II), and Hg(II) ions at low concentration levels (100-700 ppb) from aqueous solutions using three different cellulose fiber-based filter media. Sample A was pure cellulose fiber, Sample B was 10% activated carbon-cellulose fiber, and Sample C was cellulose fiber-glass fiber-30% activated carbon-20% amorphous titanium silicate (ATS). The samples were characterized by several physicochemical techniques. The porosity measurements using N_2 sorption isotherms revealed that Samples A and B are nonporous or macroporous materials, whereas the addition of 50% filler materials into the cellulose resulted in a microporous material. The Brunauer–Emmett–Teller (BET) surface area and pore volume of Sample C were found to be 320.34 m^2/g and 0.162 cm^3/g, respectively. The single ion batch adsorption experiments reveal that at 700 ppb initial metal ion concentration, Sample A had removal efficiencies of 7.5, 11.5, and 13.7% for Cu(II), Pb(II), and Hg(II) ions, respectively. Sample B effectively eliminated 99.6% of Cu(II) ions compared to Pb(II) (14.2%) and Hg(II) (31.9%) ions. Cu(II) (99.37%) and Pb(II) (96.3%) ions are more efficiently removed by Sample C than Hg(II) (68.2%) ions. The X-ray photoelectron spectroscopy (XPS) wild survey spectrum revealed the presence of Cu(II), Pb(II), and Hg(II) ions in HMI-adsorbed filter media. The high-resolution C1s spectra of Samples A and B reveal the presence of -C-OH and -COOH groups on their surface, which are essential for HMIs adsorption *via* complexation reactions. Additionally, the ATS in Sample C facilitates the adsorption of Pb(II) and Hg(II) ions through ion exchange.

Keywords: *Heavy metal ions, Biosorption, Cellulose fiber, Activated carbon, Glass fiber*

1. Introduction

The necessity for clean water is of paramount importance for potable consumption and diverse applications worldwide. Its exigency and requisition have progressively escalated over the years, owing to the exhaustion and exploitation of natural water reservoirs caused by anthropogenic actions[1]. The World Health Organization (WHO) has reported that a significant number of individuals worldwide are deprived of access to safe drinking water, thereby increasing the risk of waterborne illnesses[2]. Water is known to contain a variety of pollutants, such as heavy metal ions (HMIs), oils, petroleum byproducts, plastic wastes, organic dyes, and pharmaceutical compounds[3,4]. HMIs contamination of the environment is a major issue on a global scale. The presence of metal ions in water resources can pose a significant threat to the environment, as well as to living organisms, including humans and animals. Therefore, having effective technology to deal with these metal ions in the environment is essential[5].

The removal of hazardous materials from industrial or domestic effluents has been accomplished through various unit operations, including precipitation, ion exchange, biological, electrochemical, and membrane separation techniques[6,7]. Nonetheless, it is worth noting that these techniques exhibit certain constraints, including the requirement for a substantial quantity of reagents, the inconsistent elimination of metallic ions, and the generation of perilous sludge[8]. Adsorption is the most simple, cost-effective, efficacious, and adaptable method for removing hazardous contaminants from wastewater. The adsorption process appears to be a significant approach based on its various applications, such as user-friendliness, cost-effectiveness, wide accessibility, and uncomplicated design[9,10].

In recent years, there has been growing recognition of the potential of biosorption techniques utilizing sorbents derived from renewable resources like agricultural waste as viable alternatives to traditional methods[11,12]. The processing of agricultural resources yields substantial quantities of waste materials. Typically, the waste exhibits a substantial quantity of cellulose. Cellulose stands out as the preeminent biopolymer that is abundantly present in nature due to its non-toxicity, biocompatibility, cost-effectiveness, biodegradability, and other desirable properties[13,14]. Nevertheless, numerous hydroxyl groups in the rigid molecular chains of cellulose facilitate a robust interplay of intramolecular and intermolecular hydrogen bonding, which constrains its

† Corresponding Author: Pyeongtaek University
Department of Integrated Environmental Systems, Pyeongtaek 17869, Republic of Korea
Tel: +82-31-659-8309 e-mail: jhha@ptu.ac.kr

pISSN: 1225-0112 eISSN: 2288-4505

solubility. Cellulose, owing to its structural arrangement comprising repetitive β-D-glucose units, demonstrates a constrained adsorption efficiency due to its inability to readily establish enduring coordination complexes with HMIs. The preparation of recyclable new green functional composites is of utmost importance, with a common method being the utilization of natural polymer cellulose as the matrix. This involves combining cellulose with either organic or inorganic substances, which has been widely employed to augment the adsorption capabilities of cellulose towards HMIs[15,16]. When submerged in a solution, bulk cellulose paper can serve as both an adsorbent and a membrane to purify liquid streams, thus offering double the benefits[17].

The utilization of carbonaceous materials in water treatment is widely acknowledged due to their exceptional characteristics, such as high specific surface area, oxygen-containing functional groups, and thermal stability[18]. However, their use is somewhat constrained by inherent drawbacks, including surface inertness, propensity for agglomeration and deactivation, and challenges associated with their separation from the water medium. Combining cellulose and carbon materials offers several advantages, including avoiding complex retrieval processes and preventing secondary pollution. As a result, cellulose/carbon composites have garnered significant interest in the field of water treatment, showcasing promising prospects for practical applications[16].

The current investigation assessed the removal efficiency of three cellulose fiber-based filter media comprised of activated carbon, glass fiber, and ATS in eliminating Cu(II), Pb(II), and Hg(II) ions at low concentration levels. Since this research is for the surface water, we conducted the research of HMIs at low concentrations. Cu(II), Pb(II), and Hg(II) ions were selected as targeted HMIs due to the significance of drinking water. It also examined the impact of the initial concentration on the percentage of removal efficiency.

2. Materials & methods

Cellulose (Sample A), activated carbon-cellulose (Sample B), and activated carbon-titanium silicate-cellulose-glass fiber (Sample C) filter media were kindly provided by ENVIONEER Co., LTD., Jecheon-Si, South Korea. $CuCl_2$ (Extra pure, 99.0%), $HgCl_2$ (Special grade, 99.5%), $PbCl_2$ (Extra pure, 98.0%) and activated carbon were purchased from Samchun Chemical., Ltd., South Korea.

2.1. Batch adsorption experiments

For the adsorption experiments, the stock solutions (1000 ppm) were prepared by dissolving $CuCl_2$, $HgCl_2$, and $PbCl_2$ in distilled water and diluted to volume with de-ionized water in a volumetric flask of 1 L. The desired 1 L solutions of three metal ions with different initial concentrations (100~700 ppb) were obtained by successive dilutions of the stock solutions. The filter media were sliced to a size of 3 × 3 centimeters, and their weight was measured. The experiments were carried out in 200 mL conical flasks equipped with rubber septum. After filter media pieces were added to the metal ion solution (100 mL), the conical flask was closed with a rubber septum, and the resultant suspensions were shaken constantly (200 rpm) in an open-air shaker (OS-4000, Jeio Tech, Korea) to ensure sufficient adsorption at ambient temperature (25 ± 2 °C). The filter media samples were then removed, and the supernatant was filtered through a 0.45 μm membrane syringe filter unit. The filtrate was analyzed to determine the concentration of residual metal ions.

The metal ion removal efficiency was calculated by the following equation

$$Removal\ Efficiency\,(\%) = \frac{(C_o - C_e)}{C_o} \times 100 \tag{1}$$

The metal ion removal capacity at equilibrium was calculated by the following equation

$$Removal\ \ Capacity\,(mg/g) = (C_o - C_e) \times \frac{V}{m} \tag{2}$$

Where C_o and C_e are the initial and equilibrium concentrations in mg/L of metal ions, V is the volume of solution in Litters and m is the mass of adsorbent in grams.

2.2. Instrumentation

Fourier transform infrared (FTIR) spectra was recorded over a wavelength of 400~4000 cm^{-1} on an IRSpirit spectrometer (Shimadzu, Japan) at room temperature with a 1.0 cm^{-1} resolution. The morphology of the adsorbent samples was examined with a field emission scanning electron microscope (FE-SEM, JSM-7001F, JEOL, USA). The N_2 sorption isotherms were measured at 77 K up to 1 bar pressure using a static volumetric gas adsorption system (BELSORP-max, MicrotracBEL Corp., Japan). The elemental composition on the surface of adsorbent samples was analyzed using a K-Alpha X-ray photoelectron spectrometer (XPS, Thermo Fisher Scientific, UK) equipped with a hemispherical electron analyzer and monochromatic Al Kα (1486.6 eV) radiation. Wide Survey (full-range) and high-resolution spectra for carbon region were acquired on adsorbent samples before and after heavy metal adsorption. The experimental data of high-resolution C1s spectra was deconvoluted into separate peaks using Origin Pro 9.0 software. Prior to XPS analysis, the HMIs adsorbed filter media samples were dried at 80 °C in an air oven for 18 hours. HMI analysis was performed using inductively coupled plasma mass spectrometry (ICP-MS, Agilent 7800, Agilent Technologies, USA).

3. Results & discussion

Figure 1 displays the visual representations of the cellulose-fiber-based filter media, while Table 1 presents a comprehensive tabulation of their respective ingredients. The filter media were fabricated utilizing the wet-laid technique. In this process, fiber aggregates were formed as a thin sheet by dispersing various fiber materials and other additives in water at low concentrations according to the raw material mixing ratio. Sample A was obtained from a source consisting solely of cellulose. Sample B was produced through the combination of 10% activated carbon and cellulose. On the other hand, Sample C was pro-

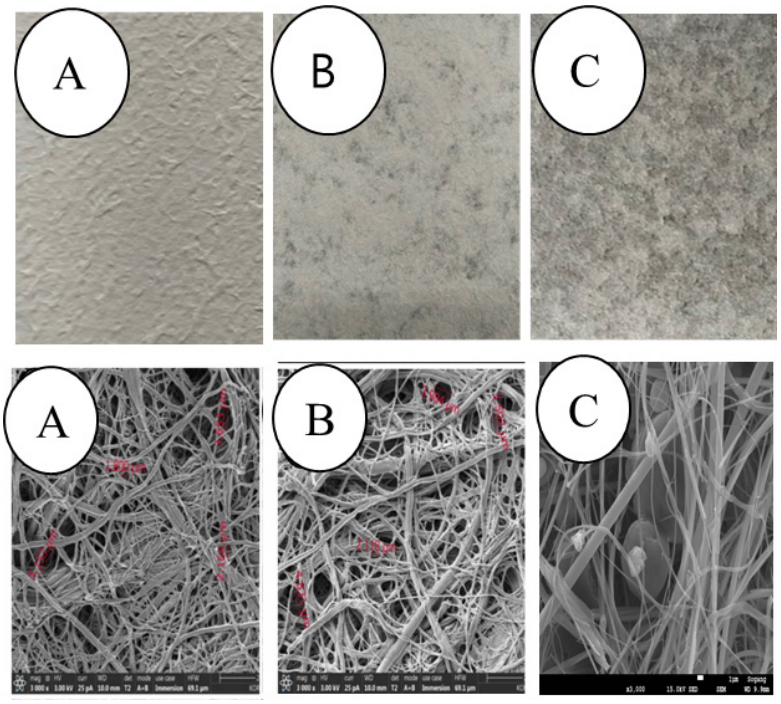

Figure 1. (Top) Images of cellulose-fiber based filter media sheets A) Sample -A; B) Sample -B C) Sample -C; (Bottom) SEM images of cellulose-fiber based filter media. A) Sample -A; B) Sample -B C) Sample -C (The SEM images were enlarged 10,000 times).

Table 1. Ingredients of Cellulose Based Adsorbent Media Samples

Serial number	Adsorbent	Ingredients
1	Sample -A	Cellulose
2	Sample -B	Cellulose, Activated Carbon (10%)
3	Sample -C	Cellulose, Glass Fiber, Activated Carbon (30%), ATS (20%)

duced by incorporating 30% activated carbon, 20% commercial amorphous titanium silicate (ATS), cellulose, and glass fiber. The main purpose of employing activated carbon is to efficiently remove organic contaminants, as well as HMIs. Filters containing glass fiber (GF) are commonly used as either a primary filter or a prefilter when sampling natural water bodies and conducting laboratory experiments that involve substantial amounts of suspended solids[19]. On the contrary, the incorporation of GF serves to augment the stability of the composite material. In a prior investigation conducted by Kahl *et al.*, it was observed that the incorporation of glass fibers into composite materials resulted in a significant improvement in tensile strength compared to composites containing cellulose fibers[20]. Furthermore, the incorporation of glass fiber into the composite not only enhances its tensile strength but also enables the adsorption of HMIs. In their study, Fuhrmann *et al.* reported that the surfactant-free cellulose acetate (SFCA), in conjunction with glass fiber filters manufactured by Cole-Parmer and Whatman, exhibited the capability to adsorb nearly all the Pb and Ag ions present in solutions with concentrations of 0.054 and 0.093 mM, respectively[19]. ATS is a cationic exchanger that is commercially manufactured by BASF. Its primary function is removing lead, mercury, and other HMIs[21]. The Scanning Electron Microscope (SEM) images in Figure 1 indicate that the adsorbent samples possess a high degree of porosity and exhibit a random stack formation characterized by irregular voids. The ATS particles are observable within the interstitial spaces of Sample C. The obtained results demonstrate a high level of concordance with previously reported cellulose and glass fiber adsorbent media[22,23].

The FTIR spectra of the three filter media samples are illustrated in Figure 2a. Sample A exhibits a wide spectral band within the 3231~3443 cm^{-1} range, indicating the presence of hydroxyl (-OH) groups. The observed peak at 2800 cm^{-1} is attributed to the stretching vibrations of $-CH_2$ groups. The observed peaks at 1050 cm^{-1} and 1308 cm^{-1} can be attributed to the stretching vibrations of C-O-C bonds in ether groups and the bending vibrations of -COO groups[24]. Sample B exhibits a comparable peak pattern to Sample A, albeit with slightly diminished intensities. Sample C exhibits a prominent and wide primary peak at 1010 cm^{-1}. The presence of the oxygen-silicon bond within the Si-O-Si group of the glass fiber can be observed at a wavenumber of 1000 cm^{-1}[25]. It was observed that the vibrations caused by stretching of C-O-C and Si-O-Si in cellulose and glass fiber exhibited significant overlap.

The porosity parameters were determined by the N_2 sorption iso-

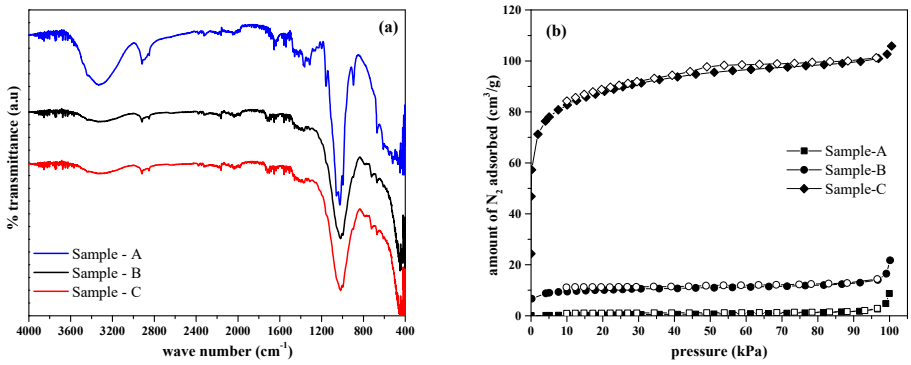

Figure 2. (a) FTIR images of cellulose-fiber based filter media; (b) N_2 sorption isotherms measured at 77 K (filled symbols represents adsorption, empty symbols represent desorption).

therms measured at 77 K, which are depicted in Figure 2b. According to IUPAC classification, Sample A and Sample B show type II sorption isotherms, characteristic of nonporous or macroporous adsorbents, whereas Sample C exhibits a type I sorption isotherm, characteristic of microporous adsorbents[26]. The BET surface areas calculated for Samples A, B, and C are 1.601, 37.127, and 320.34 m^2/g, respectively. The total pore volumes obtained for Samples A, B, and C are 0.012, 0.033, and 0.162 cm^3/g, respectively. The mean pore diameter values obtained for Samples A, B, and C are 28.92, 3.52, and 2.02 nm, respectively. Irregular voids have been clearly visible in the SEM image of Sample A, and the high mean pore diameter and negligible surface area and pore volume values suggest that macropores were formed in this cellulose fiber. Lu *et al.* reported a similar type II isotherm for cellulose fiber[27]. According to Bismarck *et al.*, the specific surface area of dehydrated cellulose varied between 0.6 and 1 m^2/g. The surface area determined for Sample A was closely consistent with this observation[28]. The interaction between the pore walls of Sample A and N_2 adsorbate molecules is negligible in this case. The addition of activated carbon reduces the mean pore diameter of the voids, and weak interactions between the pore walls of Sample B and N_2 molecules may be possible in this case. As a result, the surface area was slightly increased in Sample B, which is also macroporous. A Similar enhancement in surface area was observed in the case of MWCNT/Cellulose fiber composite[27]. The addition of ATS and activated carbon greatly reduces the mean pore diameter of Sample C, and the formation of secondary micropores between the fiber void walls, as well as ATS / activated carbon particles, is possible. The increase in the amount of N_2 adsorption might be due to the strong interactions between the pore walls of Sample C and N_2 molecules; hence, the surface area was greatly increased in Sample C.

XPS is a surface-sensitive analytical method wherein the sample is subjected to soft x-ray irradiation (energies below 6 keV), and the kinetic energy of the emitted electrons is measured. This method is considered a powerful analytical technique due to its high surface sensitivity and its capability to provide chemical state information of the elements present in the sample[29]. It was employed to analyze the chemical surface composition of three adsorbent samples. 50 ppm ternary mixture of Cu(II) + Pb(II) + Hg(II) ions was used to obtain data for after adsorption. The low-resolution complete survey (wide survey) and high-resolution C1s spectra for each sample before and after heavy metal adsorption are depicted in Figure 3a. Upon examination of the XPS wide survey spectra of the samples prior to the adsorption of HMIs, two prominent peaks are observed at around 286~285 eV and 532~531 eV. These peaks can be attributed to carbon (C1s) and oxygen (O1s), respectively. The measured binding energy values are consistent with those previously reported in the literature[30]. The wide survey of the Sample C spectrum, before adsorption, exhibited similarities to that of Sample A in both the C1s and O1s regions. Furthermore, it displayed supplementary peaks at energy levels of 458, 102, and 1072 eV, which can be attributed to the existence of titanium (Ti2p), silicon (Si2p), and sodium (Na1s). The survey spectra obtained after the adsorption of HMIs demonstrate the presence of copper (Cu2p) at a binding energy range of 930~934 eV, lead (Pb4f) at 137~138 eV, and mercury (Hg4f) at 98~101 eV. This observation serves as additional evidence supporting the ability of the three samples to adsorb heavy metals. Furthermore, the measured binding energy values align well with those previously reported in the literature[31,32]. Following the adsorption process of heavy metals, the wide survey of Sample C revealed a notable augmentation in the intensity of the Si2p peak. This observation could be attributed to an agglomeration of ATS particles after adsorption.

The high-resolution C1s spectrum of Sample A (Figure 3b) was further subdivided into three parts, with peaks observed at 287.8, 286.4, and 284.9 eV. The peaks represent the O–C–O, C–OH, and C–C bonds found in cellulose[33]. The C-OH peak is the most prominent, and after HMIs adsorption, this peak widened. In general, -OH groups are crucial for heavy metal adsorption in cellulose, and these results indicate that -C-OH groups bind metal ions through surface complexation[34]. The high-resolution C1s spectrum of Sample B (Figure 3c) was further subdivided into four peaks; in addition to the O–C–O, C–OH, and C–C peaks found in cellulose, an additional peak at 288.96 eV was attributed to -COOH groups and was obtained from activated carbon present in Sample B[35]. Due to the complexation reaction of -COOH groups with metal ions, this peak was shifted to the lower energy side and appeared at 288.36 with increased intensity in the after-adsorption sample, indicating the formation of -COOM groups[36].

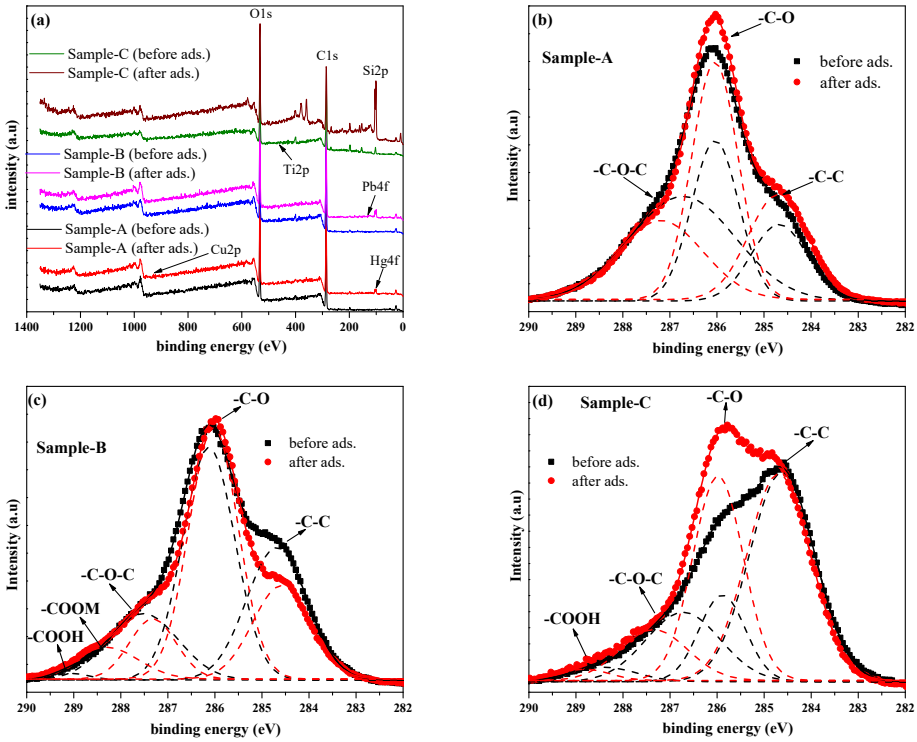

Figure 3. Comparison of XPS wide survey and high resolution C1s scan of cellulose-fiber based filter media (symbols: experimental data; solid lines: cumulative peaks; dashed lines deconvoluted peaks).

Table 2. Atomic % Values Obtained from XPS Analysis

Sample	C	O	Na	Si	Ti	Cu	Pb	Hg
Sample -A[b]	62.5	37.55	--	--	--	--	--	--
Sample -A[a]	61	37.32	--	--	--	0.1	0.01	0.15
Sample -B[b]	63.78	36.21	--	--	--	--	--	--
Sample -B[a]	60.76	38.86	--	--	--	0.1	0.27	0.01
Sample -C[b]	62.13	25.61	0.25	11.77	0.24	--	--	--
Sample -C[a]	37.12	23.48	0.16	37.52	0.14	0.08	1.42	0.03

[a] After adsorption, [b] Before adsorption

The high-resolution C1s spectrum of Sample C (Figure 3d) was further subdivided into four peaks, and its C1s spectrum was comparable to that of Sample B. Table 2 lists the atomic% values for various elements derived from XPS analysis. The oxygen atomic percentage (%) for both Sample A and Sample B increased in the sample following HMIs adsorption. This may be due to the -C-OH groups of the cellulose, which have a strong propensity to adsorb water[37]. The atomic percentage of sodium decreased following the adsorption of heavy metals in Sample C. This decrease can potentially be attributed to the exchange of Na^+ ions from ATS with metal ions.

3.1. Single ion adsorption experiments

The focus of our research lies in the enhancement of the quality of common surfacewater or natural water bodies, with the aim of rendering them suitable for human consumption. It is widely observed that the concentration of HMIs in natural water is typically found to be at low levels[38]. Consequently, the adsorption process of HMIs was conducted at low (100~700 ppb) concentration levels. Figure 4(a-c) illustrates the influence of initial concentration on the removal efficiency (%) of Cu(II), Pb(II), and Hg(II) ions on Samples A, B, and C, respectively.

The initial ion concentration is a crucial factor that promotes the transport of adsorbate ions from the bulk solution to the active binding sites of the adsorbent[39]. Sample A exhibited 55.8% removal efficiency for Hg(II) ions at 100 ppb, and removal efficiency at 700 ppb was determined to be 13.7%. At 100 ppb, the Pb(II) and Cu(II) ions removal efficiency were determined to be 22.9 and 14.7%, respectively. The removal efficiency decreased as the concentration increased. The pristine cellulose fiber filter media did not show better adsorption performance for HMIs. The -OH groups act as binding sites for HMIs, as evident from XPS analysis (Figure 3b). Sample B shows the highest removal efficiency for Cu(II) ions at all concentrations compared to Pb(II) and Hg(II) ions. It was observed that the removal efficiency val-

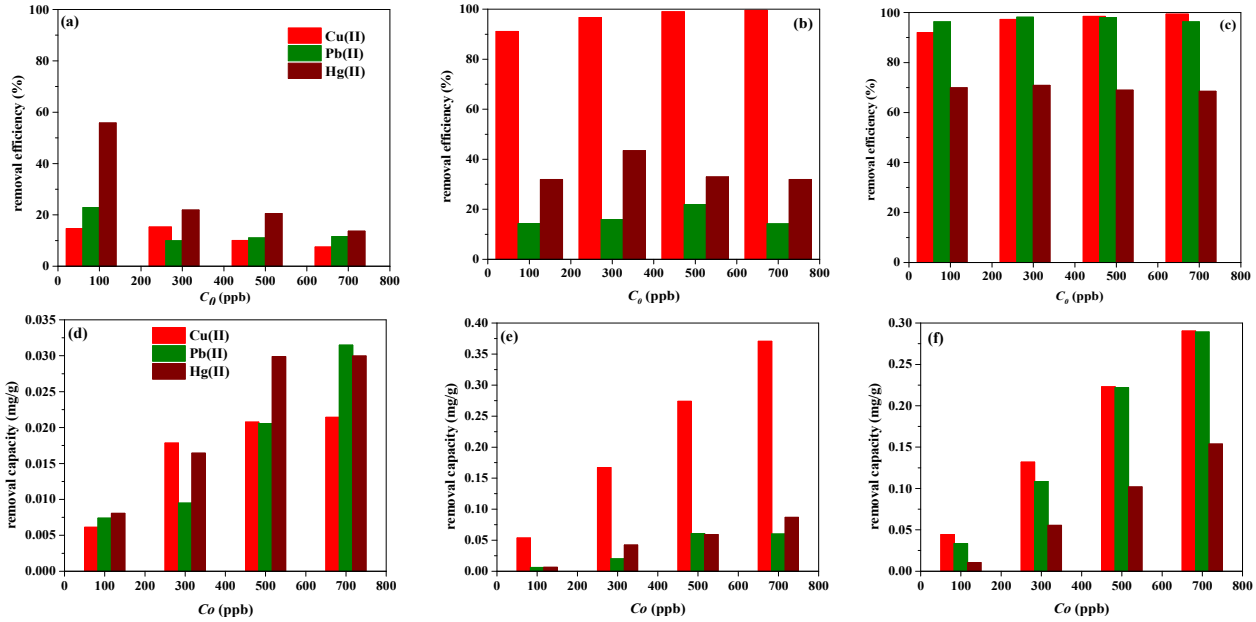

Figure 4. Effect of initial concentration on removal efficiency of Cu(II), Pb(II), and Hg(II) ions on cellulose-fiber based filter media. a) Sample A; b) Sample B; c) Sample C; Effect of initial concentration on removal capacity of Cu(II), Pb(II) and Hg(II) ions on cellulose-fiber based filter media. d) Sample A; e) Sample B; f) Sample C [volume: 100 mL; contact time: 120 minutes].

ues of Cu(II) ions at 100 and 700 ppb were 91.14 and 99.6%, respectively. The high-resolution C1s spectra of Sample B reveal the presence of -COOH groups on Sample B, and a prominent change was observed in the -COOH peak after the adsorption of HMIs (Figure 3b). Hence, it is expected that these -COOH groups act as anchoring sites for Cu(II) ions adsorption *via* surface complexation[34]. The removal efficiency values for Pb(II) and Hg(II) ions at 100 ppb were 14.3 and 31.9%, whereas at 700 ppb were found to be 14.2 and 31.9%, respectively. Sample C shows high removal efficiency for Cu(II) and Pb(II) ions. At 100 ppb, the removal efficiency values for Cu(II), Pb(II), and Hg(II) ions were determined to be 92.02%, 96.3%, and 69.9%, respectively. The removal efficiency of Pb(II) and Hg(II) remained constant at all concentrations, whereas the removal efficiency of Cu(II) ions increased slightly with increasing the initial concentration. The removal efficiency values for Cu(II), Pb(II), and Hg(II) ions at 700 ppb were 99.38, 96.3%, and 68.5%, respectively. The higher removal efficiency for Pb(II) ions on Sample C compared to other adsorbent samples was due to the presence of ion exchanger ATS, which acts as the heavy metal ion removal component[40-42]. In comparison to other samples, Sample C exhibited enhanced removal efficiency in removing Hg(II) ions, which increased by approximately 36% at 700 ppb. The observed enhancement could potentially be attributed to the presence of ATS, as indicated by prior research findings that have demonstrated the capability of ATS to adsorb Hg(II) ions [21]. The plots depicting the relationship between removal efficiency and initial concentration exhibit two distinct trends. In the case of Sample A, it can be observed that there is a decrease in removal efficiency as the concentration of Hg(II) ions increases. This phenomenon can be elucidated as follows: when the adsorbent dosage remains constant, the overall quantity of adsorption sites within the adsorbent remains constant. Consequently, the adsorbent can adsorb a nearly equivalent quantity of metal ions. As a result, the removal efficiency of the metal ions decreases proportionally with an increase in the initial concentration of the ions[43]. On the other hand, a positive correlation was observed between the removal efficiency and the concentration of Cu(II) ions in Sample B, as well as between the removal efficiency and the concentration of Pb(II) ions in Sample C. This phenomenon may be a result of a greater number of adsorption sites on the adsorbent material than metal ion concentration.

Figure 4(d-f) shows the effect of initial concentration on the removal capacity of Cu(II), Pb(II), and Hg(II) ions using Samples A, B, and C, respectively. For Sample A, the removal capacity of Pb(II) ions increased as the concentration increased from 100 to 700 ppb, and saturation was not observed in this region, whereas the removal capacity of Cu(II) and Hg(II) remained constant after 500 ppb. Cu(II), Pb(II), and Hg(II) ions removal capacities determined for Sample A at 700 ppb were 0.021, 0.031, and 0.03 mg/g, respectively. Sample B shows a higher removal capacity for Cu(II) ions, and its removal capacity was increased from 100~700 ppb, and it was not saturated in this region. Cu(II), Pb(II), and Hg(II) ions removal capacities determined for Sample A at 700 ppb were 0.37, 0.056, and 0.087 mg/g, respectively. For Sample C, the removal capacity of all three ions is increased with increasing the initial concentration from 100~700 ppb, and the removal capacity of Pb(II) ions was higher than Cu(II) and Hg(II) ions. Cu(II), Pb(II), and Hg(II) ions removal capacities determined for Sample A at 700 ppb were 0.22, 0.29, and 0.15 mg/g, respectively.

3.2. Diverse ion adsorption experiments

The filter media sheets were sliced into circles with a 4.7 cm diameter and placed in the magnetic filter funnel (47 mm diameter, PALL

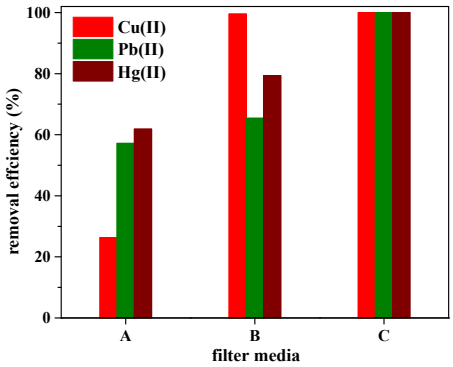

Figure 5. Removal efficiency obtained from diverse ion funnel filtration experiments using cellulose-fiber based filter media.

Corp). The funnel filtration experiments were carried out in the static mode by passing a 100 mL / 500 ppb solution of a ternary mixture of Cu(II) + Pb(II) + Hg(II) ions through Samples A, B, and C. No vacuum was applied during the filtration. The residual metal ion concentrations in the filtrate were determined, and the resultant removal efficiency values were shown in Figure 5. The obtained removal efficiency order was as follows: Sample A: Hg(II) (61.86%) > Pb(II) (57.19%) > Cu(II) (26.32%) and Sample B: Cu(II) (99.52%) > Hg(II) (79.30%) > Pb(II) (65.42%) whereas 100% removal efficiency for these three ions was achieved in the case of Sample C. Compared to single ion batch adsorption experiments, Samples A and B showed a similar trend with enhanced removal efficiency. However, Sample C demonstrated complete adsorption of Hg(II) ions in addition to Cu(II) and Pb(II) ions. In these experiments, the filter media samples were 3 × 3 cm in dimensions. Conversely, in the funnel filtration experiments, the filter media pieces had a size of 4.7 cm. The increased size, as well as the mass of the filter media samples, may account for the improved removal efficiency of these ions.

4. Conclusions

Three filter media samples fabricated with cellulose fiber (Sample A), cellulose fiber with 10% activated carbon (Sample B), and cellulose fiber with 30% activated carbon and 20% amorphous titanium silicate (ATS) (Sample C) were examined for the adsorptive removal of Cu(II), Pb(II), and Hg(II) ions at low concentration levels (100~700 ppb). The porosity measurements using N_2 sorption isotherms revealed that Samples A and B are nonporous or macroporous materials, whereas the addition of 50% filler materials into the cellulose resulted in a microporous material. The BET surface area and pore volume of Sample C were found to be 320.34 m^2/g and 0.162 cm^3/g, respectively. The single ion batch adsorption experiments reveal that, at 700 ppb initial metal ion concentration, Sample A had removal efficiencies of 7.5, 11.5, and 13.7% for Cu(II), Pb(II), and Hg(II) ions, respectively. Sample A did not show better adsorption performance for HMIs. Sample B effectively eliminated 99.6% of Cu(II) ions compared to Pb(II) (14.2%) and Hg(II) (31.9%) ions. Cu(II) (99.37%) and Pb(II) (96.3%) ions are more efficiently removed by Sample C than Hg(II) (68.2%) ions. XPS wild survey revealed the presence of Cu(II), Pb(II), and Hg(II) ions in HMIs-adsorbed filer media. The -C-OH and -COOH groups present on the surface of filter media are crucial for HMI adsorption *via* complexation reactions, as evidenced by the high-resolution C1S spectra. The higher removal efficiency for Pb(II) ions, as well as improved Hg(II) ions removal efficiency of Sample C compared to others, was due to the presence of ion exchanger ATS, which acts as the heavy metal removal component via ion exchange. In the diverse ion adsorption conducted using funnel filtration experiments, Sample C demonstrated complete adsorption of Cu(II), Pb(II), and Hg(II) ions. The increased size, as well as the mass of Sample C, may account for the enhanced removal efficiency of these ions. The utilization of ATS and activated carbon, in conjunction with environmentally sustainable biomass materials such as cellulose, in the production of composite filter media has the potential to enhance the feasibility of the HMIs removal process in the remediation of natural water bodies.

References

1. N. K. Lazaridis, G. Z. Kyzas, A. A. Vassiliou, and D. N. Bikiaris, Chitosan derivatives as biosorbents for basic dyes, *Langmuir*, **23**, 7634-7643 (2007).
2. G. S. Kumar, S. S. Kar, and A. Jain, Health and environmental sanitation in India: Issues for prioritizing control strategies, *Indian. J. Occup. Environ. Med.*, **15**, 93-96 (2011).
3. T. A. Davis, B. Volesky, and R. H. S. F. Vieira, Sargassum seaweed as biosorbent for heavy metals, *Water Res.*, **34**, 4270-4278 (2000).
4. S. E. Bailey, T. J. Olin, R. M. Bricka, and D. D. Adrian, A review of potentially low-cost sorbents for heavy metals, *Water Res.*, **33**, 2469-2479 (1999).
5. U. Farooq, J. A. Kozinski, M. A. Khan, and M. Athar, Biosorption of heavy metal ions using wheat based biosorbents-A review of the recent literature, *Bioresour. Technol.*, **101**, 5043-5053 (2010).
6. F. Fu and Q. Wang, Removal of heavy metal ions from wastewaters: A review, *J. Environ. Manage.*, **92**, 407-418 (2011).
7. D. Norton-Brandão, S. M. Scherrenberg, and J. B. V. Lier, Reclamation of used urban waters for irrigation purposes-A review of treatment technologies, *J. Environ. Manage.*, **122**, 85-98 (2013).
8. D. Lakherwal, Adsorption of heavy metals: A review, *I. J. Environ. Res. Dev.*, **4**, 41-48 (2014).
9. A. E. Burakov, E. V. Galunin, I. V. Burakova, A. E. Kucherova, S. Agarwal, A. G. Tkachev, and V. K. Gupta, Adsorption of heavy metals on conventional and nanostructured materials for wastewater treatment purposes: A review, *Ecotox. Environ. Safe.*, **148**, 702-712 (2018).
10. M. A. Barakat, New trends in removing heavy metals from industrial wastewater, *Arab. J. Chem.*, **4**, 361-377 (2011).
11. A. Demirbas, Heavy metal adsorption onto agro-based waste materials: A review, *J. Hazard. Mater.*, **157**, 220-229 (2008).
12. D. Sud, G. Mahajan, and M. P. Kaur, Agricultural waste material as potential adsorbent for sequestering heavy metal ions from aqueous solutions - A review, *Bioresour. Technol.*, **99**, 6017-6027 (2008).
13. D. Klemm, B. Heublein, H. P. Fink, and A. Bohn, Cellulose: Fascinating biopolymer and sustainable raw material, *Angew.*

Chem. Int. Ed., **44**, 3358-3393 (2005).
14. N. Tapia-Orozco, R. Ibarra-Cabrera, A. Tecante, M. Gimeno, R. Parra, and R. Garcia-Arrazola, Removal strategies for endocrine disrupting chemicals using cellulose-based materials as adsorbents: A review, *J. Environ. Chem. Eng.*, **4**, 3122-3142 (2016).
15. S. Choi and Y. Jeong, The removal of heavy metals in aqueous solution by hydroxyapatite/cellulose composite, *Fibers Polym.*, **9**, 267-270 (2008).
16. Y. -D. Dong, H. Zhang, G. -J. Zhong, G. Yao, and B. Lai, Cellulose/carbon composites and their applications in water treatment − A review, *Chem. Eng. J.*, **405**, 126980 (2021).
17. M. D. Halluin, J. Rull-Barrull, G. Bretel, C. Labrugère, E. L. Grognec, and F.- X. Felpin, Chemically modified cellulose filter paper for heavy metal remediation in water, *ACS Sustain. Chem. Eng.*, **5**, 1965-1973 (2017).
18. V. Georgakilas, J. A. Perman, J. Tucek, and R. Zboril, Broad family of carbon nanoallotropes: Classification, chemistry, and applications of fullerenes, carbon dots, nanotubes, graphene, nanodiamonds, and combined superstructures, *Chem. Rev.*, **115**, 4744-4822 (2015).
19. M. Fuhrmann and J. P. Fitts, Adsorption of trace metals on glass fiber filters, *J. Environ. Qual.*, **3**, 1943-1944 (2004).
20. C. Kahl, M. Feldmann, P. Sälzer, and H. P. Heim, Advanced short fiber composites with hybrid reinforcement and selective fiber-matrix-adhesion based on polypropylene − Characterization of mechanical properties and fiber orientation using high-resolution X-ray tomography, *Compos. Part A Appl. Sci. Manuf.*, **111**, 54-61 (2018).
21. A. D. Pronovost and M. E. Hickey, Methods and compositions for heavy metal removal and for oral delivery of desirable agents, *US Patent* 8,883,216 (2014).
22. L. Zhang, T. Tsuzuki, and X. Wang, Preparation and characterization on cellulose nanofiber film, *Materials Science Forum*, **654-656**, 1760-1763 (2010).
23. W. Li, K. Chu, and L. Liu, Multipurpose zwitterionic polymer-coated glass fiber filter for effective separation of oil−water mixtures and emulsions and removal of heavy metals, *ACS Appl. Polym. Mater.*, **3**, 1276-1284 (2021).
24. B. Abderrahim, E. Abderrahman, A. Mohamed, T. Fatima, T. Abdesselam, and O. Krim, Kinetic Thermal degradation of cellulose, polybutylene succinate and a green composite: comparative study, *World J. Environ. Eng.*, **3**, 95-110 (2015).
25. A. J. Bonon, M. Weck, E. A. Bonfante, and P. G. Coelhod, Physicochemical characterization of three fiber-reinforced epoxide-based composites for dental applications, *Mater. Sci. Eng. C*, **69**, 905-913 (2016).
26. M. M. Rahman, A. Z. Shafiullah, A. Pal, M. A. Islam, I. Jahan, and B. B. Saha, Study on optimum IUPAC adsorption isotherm models employing sensitivity of parameters for rigorous adsorption system performance evaluation, *Energies*, **14**, 7478 (2021).
27. P. Lu and Y. -L. Hsieh, Multiwalled carbon nanotube (MWCNT) reinforced cellulose fibers by electrospinning, *ACS Appl. Mater. Interfaces*, https://doi.org/10.1021/am1004128.
28. A. Bismarck, I. Aranberri-Askargorta, J. Springer, T. Lampke, B. Wielage, A. Stamboulis, I. Shenderovich, and H. -H. Limbach, Surface characterization of flax, hemp and cellulose fibers; Surface properties and the water uptake behavior, *Polym. Compos.*, **23**, 872-894 (2002).
29. F. A. Stevie and C. L. Donley, Introduction to x-ray photoelectron spectroscopy, *J. Vac. Sci. Technol.* A, **38**, 63204 (2020).
30. X. Pei, L. Gan, Z. Tong, H. Gao, S. Meng, W. Zhang, P. Wang, Y. Chen, Robust cellulose-based composite adsorption membrane for heavy metal removal, *J. Hazard. Mater.*, **406**, 124746 (2021).
31. B. Li, Y. Pan, Q. Zhang, Z. Huang, J. Liu, and H. Xiao, Porous cellulose beads reconstituted from ionic liquid for adsorption of heavy metal ions from aqueous solutions, *Cellulose*, **26**, 9163-9178 (2019).
32. Z. Hanif, S. Lee, G. H. Qasim, I. Ardiningsih, J. Kim, J. Seon, S. Han, S. Hong, and M. -H. Yoon, Polypyrrole multilayer- laminated cellulose for large-scale repeatable mercury ion removal, *J. Mater. Chem. A*, **4**, 12425-12433 (2016).
33. M. N. Belgacem, G. Czeremuszkin, S. Sapieha, and A. Gandini, Surface characterization of cellulose fibers by XPS and inverse gas chromatography, *Cellulose*, **2**, 145-157 (1995).
34. A. Salama, R. Abouzeid, W. S. Leong, J. Jeevanandam, P. Samyn, A. Dufresne, M. Bechelany, and A. Barhoum, Nanocellulose-based materials for water treatment: Adsorption, photocatalytic degradation, disinfection, antifouling, and nanofiltration, *Nanomaterials*, **11**, 3008 (2021).
35. A. Aarva, V. L. Deringer, S. Sainio, T. Laurila, and M. A. Caro, Understanding X-ray spectroscopy of carbonaceous materials by combining experiments, density functional theory, and machine learning. Part II: Quantitative fitting of spectra, *Chem. Mater.*, **31**, 9256-9267 (2019).
36. N. Li, W. Dai, H. Kang, B. Lv, P. Jiang, and W. Wang, Study on the adsorption performance and adsorption mechanism of graphene oxide by red sandstone in aqueous solution, *Adsorp. Sci. Technol.*, https://doi.org/10.1155/2022/2557107.
37. P. Sahu and M. Gupta, Water absorption behavior of cellulosic fibers polymer composites: A review on its effects and remedies, *J. Ind. Text.*, https://doi.org/10.1177/1528083720974424.
38. P. B. S. Rallapalli, S. S. Choi, H. Moradi, J. -K. Yang, J. -H. Lee, and J. H. Ha, Tris(2-benzimidazolyl)amine (NTB)-modified metal-organic framework: Preparation, characterization, and mercury ion removal studies, *Water*, **15**, 2559 (2023).
39. S. M. Ragheb, Phosphate removal from aqueous solution using slag and fly ash, *HBRC J.*, **9**, 270-275 (2013).
40. S. Kawasaki, H. Nakada, Y. Tajima, H. Yoshinobu, E. Maeda, and K. Otsuka, Composition adsorbent and method for producing thereof, and water purification material and water purifier, *US Patent* US20060163151A1 (2006).
41. A. Maglio, F. L. Himpsl, and R. V. Russo, Composite ion-exchange material preparation and use thereof, *US Patent* US5277931A (1994).
42. G. W. Dodwell and B. Smith, Removal of heavy metals, especially lead, from aqueous systems containing competing ions utilizing amorphous tin and titanium silicates, *US Patent* 5,053,139 (1991).
43. J. Das, B. S. Patra, N. Baliarsingh, and K. M. Parida, Adsorption of phosphate by layered double hydroxides in aqueous solutions, *Appl. Clay Sci.*, **32**, 252-260 (2006).

Authors

Phani Brahma Somayajulu Rallapalli; Ph.D., Post-doc, Department of Integrated Environmental Systems, Pyeongtaek University, Pyeongtaek 17869, Republic of Korea; jeonghyub@gmail.com

Jeong Hyub Ha; Ph.D., Professor, Department of Integrated Environmental Systems, Pyeongtaek University, Pyeongtaek 17869, Republic of Korea; jhha@ptu.ac.kr